

2010-01-01

Copper Isotope Fractionation During Surface Adsorption And Intracellular Incorporation By Bacteria

Jesica Urbina Navarrete

University of Texas at El Paso, jnavarrete2@miners.utep.edu

Follow this and additional works at: https://digitalcommons.utep.edu/open_etd



Part of the [Biogeochemistry Commons](#), [Geochemistry Commons](#), and the [Microbiology Commons](#)

Recommended Citation

Navarrete, Jesica Urbina, "Copper Isotope Fractionation During Surface Adsorption And Intracellular Incorporation By Bacteria" (2010). *Open Access Theses & Dissertations*. 2553.
https://digitalcommons.utep.edu/open_etd/2553

This is brought to you for free and open access by DigitalCommons@UTEP. It has been accepted for inclusion in Open Access Theses & Dissertations by an authorized administrator of DigitalCommons@UTEP. For more information, please contact lweber@utep.edu.

COPPER ISOTOPE FRACTIONATION DURING SURFACE ADSORPTION
AND INTRACELLULAR INCORPORATION BY BACTERIA

JESICA URBINA NAVARRETE

Environmental Science Program

APPROVED:

David Borrok, Ph.D., Chair

Jasper G. Konter, Ph.D.

Joanne T. Ellzey, Ph.D.

Patricia D. Witherspoon, Ph.D.
Dean of the Graduate School

Copyright

by

Jesica Urbina Navarrete

2010

COPPER ISOTOPE FRACTIONATION DURING SURFACE ADSORPTION
AND INTRACELLULAR INCORPORATION BY BACTERIA

by

JESICA URBINA NAVARRETE, B.S.

THESIS

Presented to the Faculty of the Graduate School of

The University of Texas at El Paso

in Partial Fulfillment

of the Requirements

for the Degree of

MASTER OF SCIENCE

Department of Environmental Science

THE UNIVERSITY OF TEXAS AT EL PASO

August 2010

Acknowledgements

This publication was made possible through funding by the National Science Foundation (NSF) grant 0745345, the Center for Earth and Environmental Isotope Research (NSF MRI grant 0820986) and by grant number 2G12RR008124-16A1 from the National Center for Research Resources (NCRR), a component of the National Institutes of Health (NIH). Transmission electron microscopy was provided by the Analytical Cytology Core Facility at the Border Biomedical Research Center at UTEP funded by NIH grant # 2G12RR08124-16A1. The publication contents are solely the responsibility of the authors and do not necessarily represent the official views of NCRR or NIH. Graduate funding for J. Navarrete was provided through the University of Texas System *Louis Stokes Alliance for Minority Participation* (LSAMP), NSF Grant HRD-0832951. I would like to thank Jasper G. Konter and Ming-Hua Ren for their support during the development of this manuscript.

Abstract

Copper isotopes may prove to be a useful tool for investigating bacteria-metal interactions recorded in natural waters, soils, and rocks. However, experimental data that constrain Cu isotope fractionation in biologic systems are limited and unclear. In this study we utilized Cu isotopes ($\delta^{65}\text{Cu}$) as a tool to investigate Cu-bacteria interactions, including surface adsorption and intracellular incorporation. Experiments were conducted with individual Gram-positive (*Bacillus subtilis*) and Gram-negative (*Escherichia coli*) bacterial species as well as with bacterial consortia from several natural environments. Adsorption experiments were conducted with live or dead cells over the pH range 2.5 to 6. Surface adsorption of Cu onto live bacteria cells resulted in apparent separation factors ($\Delta^{65}\text{Cu}_{\text{solution-solid}} = \delta^{65}\text{Cu}_{\text{solution}} - \delta^{65}\text{Cu}_{\text{solid}}$) ranging from +0.3‰ to +1.4‰ for *B. subtilis* and +0.2‰ to +2.6‰ for *E. coli*. The preference of the lighter Cu isotope by the cells appears to be metabolically-driven, as heat-killed bacterial cells did not significantly fractionate Cu isotopes. For the intracellular incorporation experiments, all bacteria and consortia were grown in a basal media amended with Cu(II)-citrate. The bacteria and consortia preferentially incorporated the lighter Cu isotope with an apparent $\Delta^{65}\text{Cu}_{\text{solution-solid}}$ ranging from $\sim +1.0\text{‰}$ to +4.4‰. Our results indicate that live bacterial cells preferentially sequester the lighter Cu isotope regardless of the experimental conditions. The mechanisms involved are likely related to the active cellular transport and regulation of Cu. Hence, Cu isotopes may prove to be a powerful chemical tool for probing molecular-scale bacteria-Cu interactions. Cu isotopes in natural systems may also be used to distinguish microbial activity from abiotic geochemical reactions.

Table of Contents

Acknowledgements.....	iv
Abstract.....	v
Table of Contents.....	vi
Figure Captions.....	viii
Introduction.....	1
Chapter 1: Methods.....	3
1.1 Cu-Bacteria Surface Adsorption Experiments.....	3
1.1.1 pH Dependent Adsorption Experiments.....	4
1.1.2 Metal Loading Experiments.....	5
1.1.3 Kinetics and Equilibrium Experiments.....	5
1.1.4 Control Experiments without Bacteria.....	6
1.2 Metabolic Uptake Experiments.....	6
1.2.1 Cell Washing Experiments.....	6
1.2.2 Intracellular Incorporation Experiments.....	7
1.3 ICP-OES and UV-VIS Measurements.....	8
1.4 TEM Analysis.....	9
1.5 Isotopic Analysis.....	10
Chapter 2: Results and Discussion.....	12
2.1 Adsorption Experiments.....	12
2.2 Kinetics and Reversibility Experiments.....	15
2.3. Washing Experiments.....	17

2.4 Intracellular Incorporation Experiments.....	18
2.5 Sites of Cu Accumulation and Impact on Cell Morphology.....	21
2.6 Mechanisms of Cu Isotope Fractionation	24
 Chapter 3: Conclusions.....	 27
References.....	29
Appendix.....	34
Curriculum Vita.....	37

Figure Captions

Figure 1: Copper adsorption/precipitation experiments	13
Figure 2: Copper loading experiments	14
Figure 3: Adsorption onto heat-killed cells	15
Figure 4: Kinetics of Cu adsorption	16
Figure 5: Kinetics and reversibility of <i>E. coli</i>	17
Figure 6: Kinetics and reversibility of <i>B. subtilis</i>	18
Figure 7: Washes for pre-metabolic uptake experiments	19
Figure 8: Solubility of copper citrate	20
Figure 9: Molecular structure of Cu(II)-citrate.....	21
Figure 10: Bacterial growth curves and fractionation	22
Figure 11: Transmission electron micrographs of <i>E. coli</i>	23
Figure 12: Transmission electron micrograph of <i>B. subtilis</i>	24
Figure 13: Transmission electron micrographs of <i>E. coli</i> cells grown in basal media.....	25
Figure 14: $\Delta^{65}\text{Cu}_{\text{solution-solid}}$ calculated for all experiments	27

Introduction

The stable isotopes of copper (Cu) can be used to investigate linkages between the geosphere and biosphere. Copper isotopes are substantially fractionated during abiotic chemical reactions such as surface adsorption (Balistrieri et al., 2008; Pokrovsky et al., 2008), aqueous complexation (e.g., Zhu et al., 2002; Archer et al., 2008), and oxidation/reduction reactions (e.g., Zhu et al., 2002; Erchlich et al., 2004). The latter mechanism is reflected in the isotopic variation reported among Cu⁰-, Cu(I)- and Cu(II)-bearing minerals in nature (e.g., Larson et al., 2003; Markl et al., 2006; Asael et al., 2007; Mathur et al., 2009).

Reactions with biological components also fractionate Cu isotopes; however, the magnitudes and directions of biologic fractionations and the processes that underpin them remain unclear. For example, Pokrovsky et al. (2008) found that in several cases Cu isotopes were not fractionated substantially during surface adsorption reactions with bacteria; however, one bacterial species preferentially sorbed the lighter Cu isotope. In contrast, Mathur et al. (2005) and Kimball et al. (2009) suggested that the heavier Cu isotope was preferentially sequestered by *Acidithiobacillus ferrooxidans* cells coated by iron-(oxy)hydroxides. It was not possible in this case, however, to distinguish between the adsorption of Cu onto cell surfaces versus co-precipitation with (and adsorption onto) the mineral coatings. Zhu et al. (2002) measured the isotopic changes of Cu(II) during its incorporation into proteins synthesized by bacteria and yeast. They found that the selected proteins preferentially incorporated the lighter Cu isotope and that in some cases this incorporation involved the reduction of Cu(II) to Cu(I). Buchl, et al. (2008) demonstrated that inactivation of a metal-binding prion protein in the brains of mice resulted in preferential uptake of the heavier Cu isotope relative to brain tissue with unaltered proteins.

Part of the existing ambiguity associated with Cu isotope results from biologic experiments is attributable to the fact that individual biochemical reactions are not easily isolated. Specifically, the fractionation of Cu isotopes during reversible cellular-surface adsorption has not been adequately distinguished from reactions involving intra-cellular incorporation of Cu (a problem also identified by

Wasylenki et al. (2007) for Fe and Mo interactions with bacteria). Bacterial cells contain negatively-charged organic acid functional groups that readily form complexes with aqueous metal cations like Cu (e.g., Beveridge and Fyfe, 1985; Beveridge, 1989). These surface reactions are thought to be fully reversible and have been described using surface complexation models (e.g., Fein et al., 1997). Bacterial surface-metal complexation reactions are analogous in many ways to the complexation of Cu by dissolved humic substances, as the metal-organic complexes that form in both cases are chemically and structurally similar (e.g., Ma et al., 1999; Meador, 1991; Borrok and Fein, 2004; Ashworth and Alloway, 2007). In addition to forming surface complexes with bacterial cells, Cu can be transported from the surface and into the cell where it is used in small amounts for metabolic processes and enzyme function (e.g., Brand et al., 1983; Peña, et al 1999, Finney and O'Halloran, 2003). However, at higher concentrations, Cu is toxic to the cells and can lead to the production of hydroxyl radicals and/or the structural displacement of necessary metals like calcium and magnesium (Beveridge and Koval, 1981; Koch et al., 1997).

In this study, we evaluated the Cu isotopic fractionation behavior for arguably two of the most important and ubiquitous biological interactions with metals in natural systems; surface adsorption and intracellular uptake. We performed batch Cu-adsorption and Cu-uptake experiments using individual Gram-positive (*Bacillus subtilis*) and Gram-negative (*Escherichia coli*) bacteria, as well as a variety of natural consortia of microorganisms. Care was taken to isolate surface reactions from intracellular uptake such that isotopic changes associated with both processes could be independently quantified.

Chapter 1: Methods

All media and reagents were prepared using >18M Ω ultra-pure reagent-grade water, and were sterilized in an autoclave prior to use. Reaction vessels, sample bottles, and pipette tips were acid-washed overnight in a sub-boiling solution of 10% HCl and rinsed 3 times with pure water prior to use. Ultra-pure trace metal grade acids and bases were used for experiments and sample preparation.

1.1 Cu-Bacteria Surface Adsorption Experiments

Escherichia coli and *Bacillus subtilis*, Gram-negative and Gram-positive species, respectively, were the sole focus of the Cu surface adsorption experiments. These bacteria were grown in Trypticase Soy Broth (TSB) with 0.5% yeast extract for a period of 24 hrs until growth reached mid-log phase and then were harvested and washed for experiments. Bacteria were harvested by centrifugation at 3800g and then washed 5 times in 0.01M NaClO₄ (the experimental electrolyte) to remove any residual media (e.g., Borrok and Fein, 2005). Each washing step involved suspension of the bacteria in fresh electrolyte followed by separation of the electrolyte from the cells via centrifugation. After the fifth and final wash the bacterial pellet was centrifuged at 5000g for 1 hr (supernatant was decanted during this process several times) and the moist mass of the pellet was determined. The moist mass to dry mass ratio for both cell types was about 15 to 1. The moist mass is presented here. The supernatant from the final wash was collected and analyzed using an ICP-OES technique. No measurable Cu was detected within the detection limit of ~5 μ g/L of Cu. In hindsight, the choice of a sodium-rich electrolyte was a poor one for isotope work, as the ²³Na⁴⁰Ar polyatomic combination directly interferes with ⁶³Cu. This complexity was overcome by the isotopic preparation steps described below.

Five types of adsorption experiments were conducted, 1) pH-dependent adsorption at different Cu/bacteria ratios using live cells, 2) pH-dependent adsorption at constant Cu/bacteria ratio using dead cells, 3) Cu loading at a constant pH with live cells, 4) Adsorption kinetics and reversibility with live cells, and 5) Control experiments without bacteria. All adsorption experiments were conducted under

chemical conditions (e.g., pH range) where non-ligand bound aqueous Cu(II) was the dominant (>95%) form of Cu in solution (in the absence of bacterial surface complexes) as confirmed by modeling of the experimental conditions using Visual Minteq ver. 2.53 (Gustafson 2007). Copper(II) diluted from an in-house atomic adsorption standard was used for all the adsorption experiments.

1.1.1 pH-Dependent Adsorption Experiments

Batch adsorption experiments were conducted with *E. coli* and *B. subtilis* in stock solutions of 0.01M NaClO₄ with component ratios of moist bacteria (in g) to Cu(II) (in mg/L) of 5:10 and 15:2. These component ratios were chosen to highlight possible differences in the Cu-organic complexation chemistries of the different functional group sites that might bind Cu. Thirty mL aliquots of the homogeneous bacteria-Cu stock suspensions were collected and placed in batch reaction vessels. The pH of each vessel was individually adjusted to values between 2.5 and 6.5 using 0.2 mL aliquots of 0.1N HNO₃ or 0.2N NaOH. The experimental batches were allowed to equilibrate on a shaker table for 1 hour after which the equilibrium pH was measured. The equilibration time was determined using the kinetic information described below. The reaction vessels were centrifuged and filtered with a pre-cleaned 0.45μM nylon syringe filter to separate the bacterial pellets from the supernatant. Control experiments confirmed that Cu did not interact with the filter (data not shown).

The supernatant was preserved through acidification by adding 0.5 mL of concentrated ultrapure HNO₃ and then analyzed for its Cu content using the ICP-OES method. A split from each sample was used for Cu isotopic analysis. Adsorption of Cu onto the bacterial pellet was determined by the difference between the initial Cu concentration of the stock solution and the amount of Cu remaining in solution after filtration.

The same experimental procedure was followed for adsorption of Cu onto dead *E. coli* cells. *E. coli* cells were heat-killed by placing the bacteria-electrolyte stock solution in a hot water bath where the temperature was slowly raised. After extensive testing, we found that the minimum effective

temperature and time necessary to kill but not lyse the *E. coli* cells was 40°C for 15 minutes. After this point we could not achieve any bacterial growth by streaking TSA plates. The cellular integrity of the heat-killed *E. coli* was verified through microscopic examination of Gram- stained cells.

1.1.2 Metal Loading Experiments

Metal loading experiments were conducted to test whether isotopic fractionation of Cu changed as available functional group sites become saturated with Cu at a single pH. First, a stock solution of 5g/L of bacteria in a 0.01M NaClO₄ was prepared and adjusted to pH= 4 using a few mL of 0.1N HNO₃. The solution was stirred using a magnetic stirring rod (raised 1 inch from the bottom of the vessel with a plastic mounting device) and the pH was held constant with a Radiometer TIM 856 autotitrator/pH-stat instrument. Copper was added to the stock solution in 1 hour steps to achieve concentrations of 5, 10, 25, 50, and 100 mg/L. Each addition of Cu was followed by a 1 hour equilibration time. After equilibration, 30 mL samples of the homogeneous suspension were collected using a sterile, pre-rinsed serological pipette and filtered through a pre-cleaned 0.45µm nylon filter. The filtrate was acidified for preservation and analyzed for its Cu content and a sample split was processed for isotopic analysis.

1.1.3 Kinetics and Equilibrium Experiments

Kinetics experiments were conducted with both laboratory bacterial strains. A stock solution of 5g/L bacteria and 10 mg/L of Cu in 0.01M NaClO₄ was held at a constant pH of 4.3 using the pH-stat instrument. Thirty mL samples of the homogeneous mixture were collected after about 5, 15, 30, 60, and 80 minutes, 25 hours, and 48 hours. Each sample was filtered through a pre-cleaned 0.45µm nylon syringe filter; the filtrate was acidified and analyzed for its metal content on the ICP-OES and a split of the sample was prepared for isotopic analysis. Reversibility experiments were conducted to test whether Cu adsorption onto surface functional group sites was an equilibrium process. A stock solution of 5g/L bacteria and 10 mg/L of Cu in 0.01M NaClO₄ was held at a constant pH of 4.0 for three hours before

being adjusted to pH= 5.0 (using 0.2N NaOH). After 2 hours at pH=5, the solution was adjusted back to pH = 4.0 using 0.2N HNO₃ where it was held constant for two more hours. At the beginning of the experiment and after each pH change, 30 mL samples were collected at approximately 1, 5, 15, 30, 60, 90, 120 and 180 minutes. One additional sample was collected after 24 hours at the final pH of 4. Samples were processed as described above.

1.1.4 Control Experiments without Bacteria

All procedures followed for the pH-dependent adsorption experiments at constant Cu/bacteria ratio were duplicated for the control experiment with the exception that bacteria were not added. The objectives of this experiment were to verify that Cu did not sorb to the filter or experimental apparatus and that Cu was soluble over the pH range predicted by thermodynamic modeling.

1.2 Metabolic uptake experiments

1.2.1 Cell Washing Experiments

In order to verify that we could successfully isolate intracellular Cu from surface-bound Cu, we performed a series of washing experiments. The first set of washing experiments focused on the removal of surface adsorbed Cu(II) from *E. coli* and *B. subtilis*. The second set of experiments focused on the removal of Cu(II)-citrate from solutions in contact with these same bacteria. The wash experiments were carried out using a series of solutions of varying pH and ionic strength designed to remove Cu but not damage the integrity of the cell walls. Each experiment was subjected to 5 washing cycles consisting of centrifugation and then re-suspension in fresh wash solution. The supernatant from the individual wash cycles was collected and analyzed using an ICP-OES and Dissolved Organic Carbon (DOC) analyzer to determine Cu and DOC concentrations, respectively. The latter analyses confirmed that cells were not lysed during the washing experiments (data not shown). Optical microscopy and TEM images confirmed that the cells remained intact after washes.

1.2.2. Intracellular Incorporation Experiments

For the intracellular incorporation experiments we additionally used natural consortia of microorganisms collected from the Rio Grande Reservoir (RGR) and Cement Creek (CC) in Southwest Colorado. The RGR was characterized by high pH (~10), moderate human and water fowl activity, high DOC content, and turbid water. Cement Creek is a mountain stream rich in Fe and other metals derived from acid rock drainage. The CC site was characterized by low pH (~3.7), high conductivity ($>1600 \mu\text{S}\cdot\text{m}^{-1}$) and high levels of dissolved Fe(II), Cu(II), and Zn(II). Both samples of wild-type microorganisms were characterized by Gram-staining with light microscopy. The RGR consortia included fungi, diatoms, and protozoa, as well as Gram-positive and Gram-negative bacteria of differing morphologies (cocci, bacilli, vibrio). The CC consortia contained Gram-negative rods, Gram-positive cocci, and some fungi.

Experiments were performed by growing bacteria in a specially-formulated basal medium amended with Cu(II)-citrate. The media recipe followed that for “FeDM” described by Hersman et al. (2001) and contained the following per L of 18M Ω pure water: 1g glucose, 0.5g K₂HPO₄, 1.0g NH₄Cl, 0.2g MgSO₄*7H₂O, 0.2g CaCl₂*2H₂O, 8.33g succinate disodium salt, 30mM Fe-EDTA, 4.77g HEPES buffer, and 0.125mL of additional trace elements (5mg MnSO₄*H₂O, 6.5mg CoSO₄*7H₂O, 3.3mg ZnSO₄ and 2.4mg MoO₃). Prior to the addition of Cu(II)-citrate, the basal media was analyzed for its trace element content and had no Cu ($<0.005 \text{ mg/L}$). The basal media was amended with 3 mg/L Cu(II)-citrate (about 1 mg/L Cu) for each bacterial experiment and control experiments were performed with bacteria with no added Cu and with Cu but no bacteria. Cu(II)-citrate was chosen because the aqueous citrate complex keeps Cu(II) from reacting with the cell surface functional group sites but still allows for the uptake of Cu(II) into the cells. Control experiments verified the aqueous stability of the Cu(II)-citrate complex and that this complex did not react with the bacterial surface (see results section).

The different bacterial strains and consortia were grown in the basal media amended with Cu(II)-citrate until they reached mid-log phase (UV-VIS measurements). At this stage the cells were harvested via centrifugation. Harvested cells were washed three times with a solution of 0.2M MgSO₄ at pH 1.5 (e.g., Cheng et al., 1970). Cells were digested with a mixture of 70% HNO₃ and 30% H₂O₂, evaporated to dryness and re-dissolved in 2% nitric acid. This solution was analyzed for its copper content using an ICP-OES and sample splits were prepared for isotopic analysis.

1.3 ICP-OES and UV-VIS Measurements

The supernatant from all adsorption and control experiments, as well as the bacterial digests from the intracellular uptake experiments were analyzed for their Cu concentrations using a Perkin-Elmer Optima 5300DV ICP-OES instrument. Standards were diluted from a CertiSPEX® multi-element standard. Uncertainty was quantified through replicate analyses and was found to be less than $\pm 5\%$. USGS standard reference waters were used as an external check to verify accuracy. Optical density measurements for bacterial growth were conducted using a Hach 2300 UV-Vis photospectrometer at a light wavelength of 600nm. Uncertainty was quantified through replicate analysis of samples and was found to be $\pm 2\%$.

1.4 TEM Analysis

Transmission electron microscope (TEM) images of bacteria before and after exposure to Cu were collected using a Zeiss EM-10 TEM in the Department of Biological Sciences Analytical Cytology Core Facility at the University of Texas at El Paso. Cells from the selected experiments were pelleted through centrifugation and then suspended in warm agar. A glutaraldehyde-osmium tetroxide fixation technique was used to prepare the specimens. These methods are similar to those described previously by Kimball et al. (2009). Agar specimens were minced with a razor blade to a size of $\sim 1\text{mm}^3$ and transferred to fixation vials where they were filled 1/3 full with 3% glutaraldehyde in 0.12M Millonig's

phosphate buffer (pH 7.4). Vials were placed in a rotary agitator at room temperature for 1 hour. Glutaraldehyde was removed from the vials and the samples were washed 3 times with fresh cold 0.06M phosphate buffer (5-15 min per wash). A solution of 1% OsO₄ in 0.12M phosphate buffer was added to cover the specimens in the vials. Vials were placed in an ice bucket (dark, 0-4°C) for 1.5hrs before the OsO₄ was removed and the specimens washed with cold 0.06M phosphate buffer 3 more times followed by 3 rinses of double distilled water. Uranyl acetate (0.5%) was added to the specimens and they were wrapped with aluminum foil and left to incubate at room temperature for 1 hour. The uranyl acetate was then removed and the sample rinsed 3 times with distilled water. Samples were dehydrated by washing with an ethanol and acetone series. Poly/Bed 812 plastic (Polysciences, Inc., Warrington, PA) was allowed to infiltrate into the samples for 6 hours, after which a drop of the plastic was placed at the bottom of a BEEM capsule. Specimens were transferred to the BEEM capsules and then 100% plastic was used to fill the remaining capsule volume. The capsule was placed in an embedding tray for at least 48hrs in a 60°C oven. Thick sections (1 µm) were stained with Toluidine Blue and Fuschin to determine suitable areas to be thin sectioned with a Leica Ultracut ultramicrotome (60-90 nm). Hardened specimens were sectioned into ~90nm sections and mounted on 200 mesh copper grids for analysis. Thin sections were post stained with uranyl acetate followed by Reynolds lead citrate. Grids were examined and photographed in a Zeiss EM-10 transmission electron microscope (Carl Zeiss SMT, Inc. Peabody, MA) operating at an accelerating voltage of 60 or 80 kV. Digital images were obtained with a Gatan 385C CCD camera.

1.5 Isotopic Analysis

Selected samples from the adsorption, control, and intracellular uptake experiments were prepared for isotopic analysis. First, Cu was isolated from the solution matrix through anion exchange chromatography as described by Borrok, et al. (2007). Savillex® Teflon beakers, pipette tips and sample storage containers were all acid-washed overnight in a sub-boiling 10% HCl bath and washed 3 times in

ultra-pure water prior to use. Column separations were performed in a Class 100 HEPA-filtered laminar flow clean bench. Column separation of Cu proved to be a relatively simple process because Cu was the only element of interest in the experiments; however, in several cases Na (from the NaClO₄ electrolyte) broke through into the Cu fraction during the initial separation. Hence, we passed the Cu fraction through the column procedure a second time for additional purification (e.g., Pribil et al., 2010). Procedural blanks revealed no measurable Cu contamination and all Cu separates were analyzed using the ICP-OES technique prior to isotopic analysis to verify quantitative elution (within analytical uncertainties of about $\pm 5\%$) and to check for possible contaminants, including sodium.

For the adsorption experiments we prepared only supernatant samples for analysis and not bacterial pellets. Because bacterial pellets remain “wet” after centrifugation, the adsorbed Cu is allowed to co-mingle with the free Cu that remains in solution. Therefore, the Cu isotopic signature of the bacterial pellet is compromised (e.g., Barling and Anbar, 2004). Instead, we calculated the $\delta^{65}\text{Cu}$ for adsorbed Cu through isotopic mass balance.

Isotopic analyses were conducted using a Nu Instruments multicollector ICP-MS at the Center for Environmental and Earth Isotopic Research (CEEIR) at UTEP. The NIST SRM 976 Cu standard was used as a reference material. The SRM standard was also passed through the column chromatography to eliminate any differences in sample matrix (e.g., Archer and Vance, 2004). All samples were evaporated to dryness after column separations and 1 mL of 2% ultrapure nitric acid was added twice and evaporated to dryness to remove residual Cl from the column chemistry. Samples, standards, and blanks were reconstituted in ultrapure 0.2% nitric acid in preparation for delivery into the MC-ICP-MS via a de-solvating nebulizer (Nu DSN 100) system. Each sample was bracketed by the SRM standard and results are presented in standard delta notation (parts per thousand) relative to the average of the two bracketing standards,

$$(1) \quad \delta^{65}\text{Cu} = \left[\frac{\frac{65}{63}\text{Cu}_{\text{sample}} - \frac{65}{63}\text{Cu}_{\text{ave std}}}{\frac{65}{63}\text{Cu}_{\text{ave std}}} \right] \times 1000.$$

Experimental results are also reported as isotopic separation factors, which are defined by the following equation:

$$(2) \quad \Delta^{65}\text{Cu}_{\text{solution-solid}} = \delta^{65}\text{Cu}_{\text{solution}} - \delta^{65}\text{Cu}_{\text{solid}}$$

Long term analytical precision was determined by replicate analyses of two in-house Cu standards, a J.T. Baker® AA standard and a digested Cu-rod obtained from a nearby Cu refinery. Each of these standards was prepared as an unknown and purified through the column chemistry procedure. Over a period of 8 months, the 2σ precision for the Cu rod standard was $\pm 0.16\text{‰}$, (n=12) and the 2σ precision of the AA standard was $\pm 0.14\text{‰}$ (n=15). The uncertainties for column duplicates fell within these ranges. Error bars reported in all figures reflect calculated 2σ uncertainties from 3 or more replicates; however, average uncertainties are reported for samples with fewer than 3 replicates. The complete Cu isotope dataset is presented in the Appendix section of this publication.

Chapter 2: Results and Discussion

2.1 Adsorption Experiments

Concentration and isotopic data for the pH-dependent adsorption experiments are presented in Figures 1a-d. In all cases the fraction of Cu adsorbed from solution increased with increasing pH over the tested pH range of 2 to 6.5. This is an expected result, because as pH increases, more bacterial-surface functional group sites become deprotonated and available to react with free Cu(II) (Beveridge and Fyfe, 1985; Beveridge, 1989; Fein et al., 1997). The control experiment without bacteria (Fig. 1a) demonstrates that no Cu precipitation or adsorption onto the reaction vessel occurred over the tested pH range. *E. coli* and *B. subtilis* adsorbed similar amounts of Cu at the same pH and experimental conditions (Figs 1b and d), while an increase in the *E. coli* : Cu(II) ratio resulted in more Cu(II) binding at lower pH (Fig. 1 c).

The $\delta^{65}\text{Cu}$ of the starting solution for all adsorption experiments was $+0.71\text{‰} \pm 0.16$; however, for illustration purposes we have normalized the adsorption data to a starting point of 0.0‰ in all figures by subtracting $+0.71\text{‰}$ from each sample. The control experimental data (Fig. 1a) demonstrate that the heavier Cu isotope is preferentially incorporated into Cu oxy-hydroxide precipitates (leaving the solution depleted in the heavy isotope) during abiotic precipitation at $\text{pH} > \sim 6.5$. During the initial stages of precipitation, the $\delta^{65}\text{Cu}$ of the solution increased slightly suggesting the possibility of a modest kinetic isotope effect followed by equilibrium fractionation.

The $\delta^{65}\text{Cu}$ of the solution in the bacterial adsorption experiments became heavier relative to the starting $\delta^{65}\text{Cu}$ (Fig 1b-d). This demonstrates that the bacterial surfaces became enriched in the lighter isotope of Cu. This observation holds true for experimental systems with variable bacteria:Cu ratios and for both strains of bacteria. The apparent separation factor for this process, $\Delta^{65}\text{Cu}_{\text{solution-solid}}$ (Eq. 2), was as large as $+2.6\text{‰}$ for the *E. coli* adsorption experiments and $+1.4\text{‰}$ for the *B. subtilis* experiment. The preferential sequestration of the lighter Cu isotope during bacterial surface adsorption was an unexpected result, as adsorption experiments with mineral surfaces have shown that the heavier Cu

isotope is preferentially incorporated into the Cu-surface complex (e.g., Balistrieri et al., 2008). The initial shift to heavier $\delta^{65}\text{Cu}$ in the solution occurs at low levels of adsorption and low pH; however, the $\delta^{65}\text{Cu}$ of the solution does not change much after about 40% adsorption (Fig. 1b-d). Because the fraction adsorbed does not correlate with the $\delta^{65}\text{Cu}$ in a consistent manner, it appears that either (1) the observed fractionations are attributable to a process unrelated to adsorption, or (2) that the observed fractionations are the result of summing of fractionations from several individual reactions governed by the differences in chemical bonding environments active under different pHs.

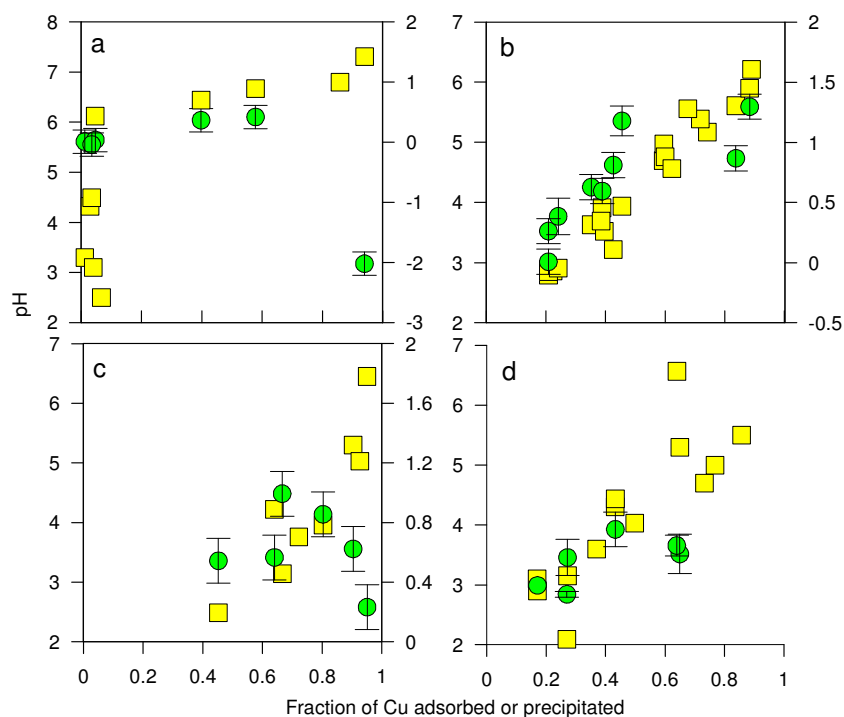


Figure 1. Cu concentration (yellow squares), $\delta^{65}\text{Cu}$ (green circles), and pH data plotted as a function of the fraction of Cu adsorbed for (a) an abiotic precipitation experiment, (b) adsorption of 10 mg/L of Cu by 5 g/L *E. coli*, (c) adsorption of 2 mg/L Cu by 15 g/L *E. coli*, and (d) adsorption of 10 mg/L Cu by 5 g/L *B. subtilis*.

The results of the metal loading experiments are presented in Figure 2a and b for *E. Coli* and *B. subtilis*, respectively. In the metal loading experiments, the pH is held constant to isolate its impact on the isotopic changes. The adsorption of Cu onto both bacterial species follows a Langmuir distribution

in that the amount of adsorption asymptotically approaches a maximum value that is a reflection of the concentration of available binding sites. Under low Cu loads, the $\delta^{65}\text{Cu}$ of the solutions become enriched in the heavier Cu isotope relative to the parent solutions, and the magnitude of the fractionation is similar to that measured for the pH-dependent experiments. The $\delta^{65}\text{Cu}$ values for the metal loading solutions begin to match the parent solution as more Cu is added and the active binding sites on the bacterial surfaces become saturated (i.e., smaller and smaller fractions of the total Cu are adsorbed). In order to estimate fractionation behavior at these high metal:bacteria ratios, we additionally analyzed the $\delta^{65}\text{Cu}$ of several digested bacteria pellets. The results (not shown) indicate that the lighter isotope of Cu is still enriched in the bacteria at high metal:bacteria ratios, but quantification of the magnitude of the fractionation was difficult because aqueous Cu was not fully removed from the cells (see section 1.5).

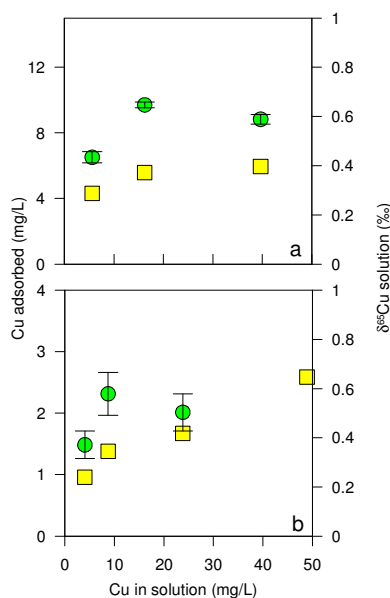


Figure 2. Cu concentration (yellow squares) and $\delta^{65}\text{Cu}$ (green circles) data for Cu-loading experiments with (a) *E. coli* and (b) *B. subtilis* at pH 4.

The cells used in adsorption experiments were considered to be “non-metabolizing” because they were carefully washed to remove nutrients and were suspended in an electrolyte solution that provided no energy. Despite these precautions we decided to test the possibility that the cells retained some stored

energy for metabolic function that impacted Cu isotopes. To this end, we performed a set of adsorption experiments with intact but heat-killed *E. coli* cells (Figure 3).

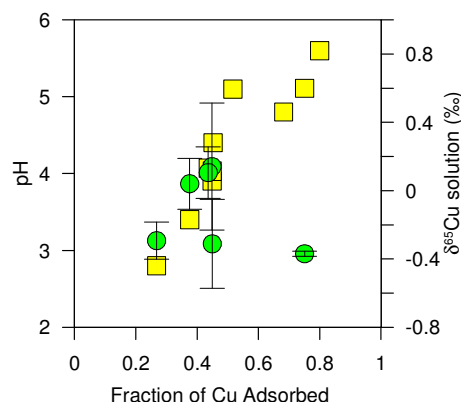


Figure 3. Cu concentration (yellow squares) and $\delta^{65}\text{Cu}$ (green circles) data plotted as a function of the fraction of Cu adsorbed for the experiment with 10 mg/L Cu and 5 g/L of dead (heat-killed) *E. coli*.

The extent of Cu adsorption onto the dead cells increased with increasing pH and the extent of Cu adsorption was similar to that of the corresponding live cell experiment (Figure 1b). The $\delta^{65}\text{Cu}$ of the solution, however, either 1) did not change substantially from the $\delta^{65}\text{Cu}$ of the starting solution (at least within the uncertainty of the analyses), or 2) indicated a slight preference for adsorption of the heavier Cu isotope. For example, at 75% adsorption of Cu onto the dead cells, the $\delta^{65}\text{Cu}$ of the solution was actually less than the starting solution by 0.37‰ (a $\Delta^{65}\text{Cu}_{\text{solution-solid}}$ of -0.49‰), suggesting that surface adsorbed Cu complexes on dead cells may show a slight preference for the heavier Cu isotope. This behavior is opposite of that observed for live cells, suggesting that preferential incorporation of light Cu isotopes was an active cellular process (presumably triggered using stored energy).

2.2 Kinetics and Reversibility Experiments

The results of the kinetics and reversibility experiments are presented in Figures 4, 5, and 6. As observed in the pH-dependent adsorption experiments, the $\delta^{65}\text{Cu}$ of the solution initially increased relative to the starting $\delta^{65}\text{Cu}$ during the kinetic experiments. Figures 4 and 5 demonstrate that the bulk of

Cu(II) adsorption onto *E. coli* occurs in the first several minutes; however, some additional Cu(II) adsorbs slowly over a period of about 12 hours (Fig. 4). The $\delta^{65}\text{Cu}$ of the experimental solutions, however, did not appreciably change despite the fluctuations in the adsorbed concentrations of Cu that occurred as time increased (Fig. 4).

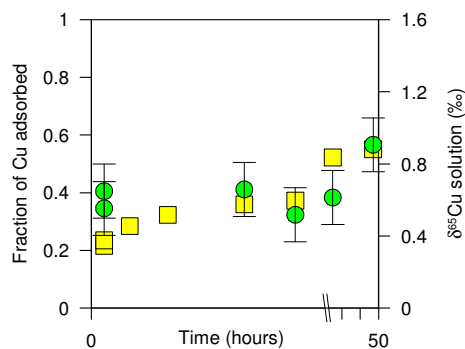


Figure 4. Cu concentration (yellow squares) and $\delta^{65}\text{Cu}$ (green circles) data plotted as a function of time for the kinetics experiment with *E. coli* (10 mg/L Cu and 5 g/L bacteria).

The extent of Cu adsorption onto *E. coli* was not fully reversible as ~20% of the Cu was adsorbed initially at pH 4, while ~30% of the Cu was adsorbed upon returning to pH 4 after the intermediate adsorption step at pH = 5 (Fig 5). The irreversible sequestration of a small amount of Cu in the *E. coli* cells was confirmed in our washing experiments as only about 60% of surface-bound Cu was recovered (Fig 7a).

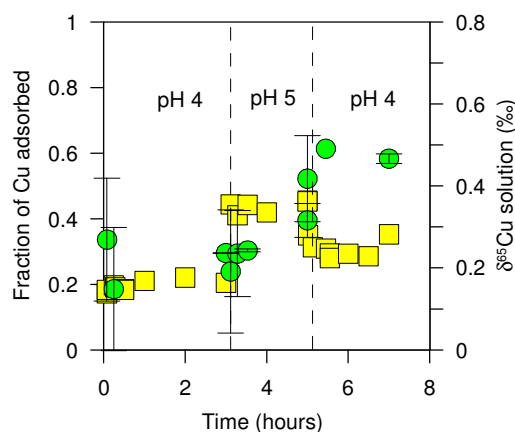


Figure 5. Cu concentration (yellow squares) and $\delta^{65}\text{Cu}$ (green circles) plotted as a function of time for the kinetics and reversibility experiment with *E. coli* (10 mg/L Cu and 5 g/L bacteria). The pH of the experiment was changed from 4 to 5 and back to 4 at the times identified by the dashed lines.

The adsorption of Cu onto *B. subtilis* cells was rapid, did not increase as a function of time (for the 2 hour period tested), and appeared to be fully reversible (Fig. 6). However, the $\delta^{65}\text{Cu}$ of the solution did not equilibrate as quickly. At the start of the experiment, the $\delta^{65}\text{Cu}$ of the solution immediately increased relative to the starting solution and increased further as a function of time during the initial pH step. This may indicate that Cu isotopes were being fractionated via a kinetic isotope effect perhaps related to transport across the cell membrane. The $\delta^{65}\text{Cu}$ of the solution did not appreciably change at the pH 5 step and remained relatively consistent as pH was changed back to 4.0 (Fig. 6). The $\delta^{65}\text{Cu}$ for each of the reversibility experiments did not significantly change in response to the pH change from 4 to 5 and back to 4 (Figs. 5 and 6). This supports the interpretation that changes in surface adsorption are not controlling the observed isotopic changes.

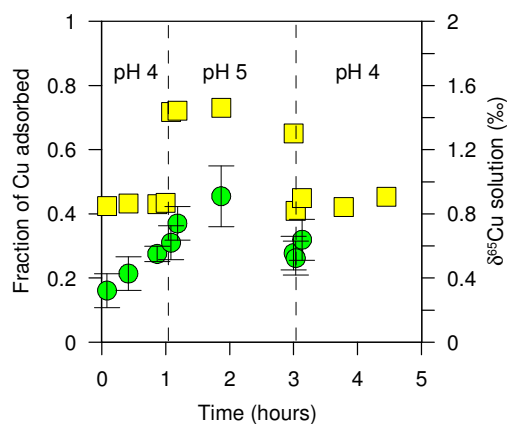


Figure 6. Cu concentration (yellow squares) and $\delta^{65}\text{Cu}$ (green circles) data plotted as a function of time for the reversibility experiment with *B. subtilis* (10 mg/L Cu and 5 g/L bacteria). The pH of the experiment was changed from 4 to 5 and back to 4 at the times identified by the dashed lines.

2.3. Washing Experiments

Washing experiments were conducted to identify the most effective method(s) for the removal of adsorbed Cu from bacterial surfaces while keeping intracellular Cu intact (Figure 7). We used 6 different chemical solutions to wash *E. coli* and *B. subtilis* after exposure to Cu(II) at pH ~ 4.5. Under this condition we expected that ~5 mg/L of Cu(II) was adsorbed to the bacterial surfaces. The most effective chemical agent for Cu removal was a simple pH = 1.5 HNO₃ solution with or without a 0.2 M MgSO₄ electrolyte. The other electrolyte solutions were slightly less effective. The pH = 1.5 washes of the *B. subtilis* cells yielded 100% \pm 5% recovery of Cu(II), while washes of *E. coli* were only effective for the recovery of 60% \pm 5% Cu(II) (Fig. 7a). This finding is confirmation of the reversibility experimental results (Fig. 5), which demonstrated that Cu(II) adsorption onto *E. coli* was not a fully reversible process.

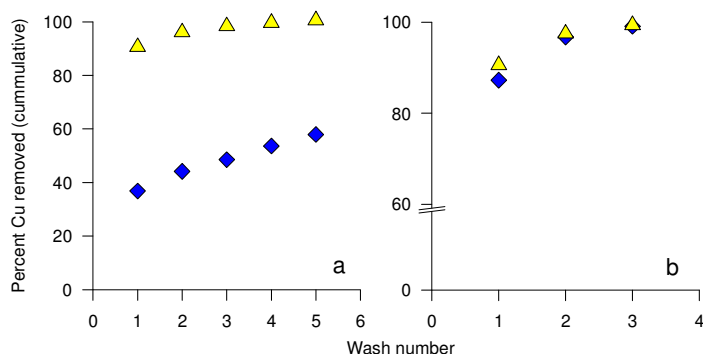


Figure 7. The cumulative percentage of adsorbed Cu removed from *B. subtilis* (yellow triangles) and *E. coli* (blue diamonds) using washes of 0.2M MgSO₄ at pH 1.5. Panel (a) depicts washes from experiments conducted with Cu(II) and panel (b) depicts washes from experiments conducted with Cu(II)-citrate.

Largely because of this irreversible binding behavior, we evaluated whether we could be successful in washing Cu(II)-citrate from the bacterial surfaces. Because Cu(II)-citrate forms a strong aqueous complex in pH-circumneutral solutions we expected that 1) Cu(II)-citrate would not bind strongly with the bacterial surface at circumneutral pH, and 2) what Cu(II)-citrate did associate with the bacterial surface would be easily removed. Figure 7b presents the results of washing experiments for Cu(II)-citrate and shows that 100% \pm 5% of the Cu was recovered from both bacterial species in the first 3 washes.

2.4 Intracellular Incorporation Experiments

Cu(II)-citrate was used for the intracellular incorporation experiments because it did not bind appreciably with the bacterial surface (see above) and we needed additional flexibility in the pH range for the growth experiments (i.e., Cu not complexed as Cu(II)-citrate would mostly precipitate under circumneutral pH conditions). Control experiments confirmed that the Cu(II)-citrate complex did not precipitate, and did not adsorb to the reaction vessels under the experimental pH conditions (Fig. 8).

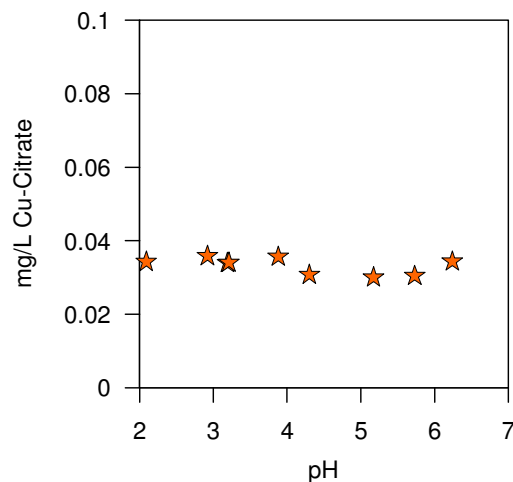


Figure 8. Concentration of Cu in Cu(II)-citrate remaining in solution after centrifugation and filtration at different pH points.

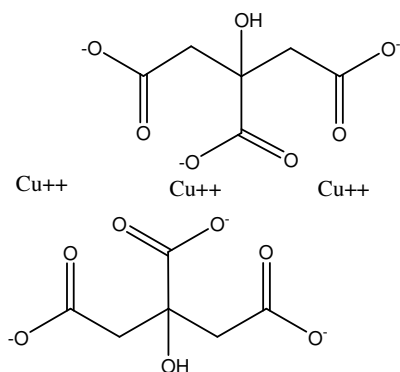


Figure 9. Molecular structure of Cu(II)-citrate.

Cu(II)-citrate $[\text{Cu}_3(\text{C}_6\text{H}_5\text{O}_7)_2]$ contains 3 Cu atoms bound to deprotonated carboxylic functional group locations, as illustrated in Figure 9 (e.g., Green et al., 1998; Ivanov and Tsakova, 2002). It is possible that the choice of Cu(II)-citrate over other possible Cu-organic complexes might have some influence on the bacterial metabolisms. However, we believe that Cu(II)-citrate is a suitable analog for Cu in natural environments because 1) free Cu(II) is all but absent in natural waters at circumneutral pH because of its propensity to hydrolyze and precipitate (e.g., Smith and Martell, 1978), and 2) most Cu

that is present is bound to dissolved organic ligands associated with dissolved humic substances that are dominated by carboxylic functional group sites (Gauthier et al., 1987).

Results for the intracellular incorporation experiments are presented in Figures 10a-d. All of the bacterial species and consortia reached exponential growth phase by day 4 of the experiments. *E. coli* (Fig. 10a), *B. subtilis* (Fig. 10b), the RGR bacterial consortium (Fig. 10c), and the CC bacterial consortium (Fig 10d) all preferentially incorporated the lighter isotope of Cu during growth. Although the direction of the isotopic fractionation was consistent for all experiments, the magnitude of the fractionation (relative to the starting solution) was dependent on the species and consortium.

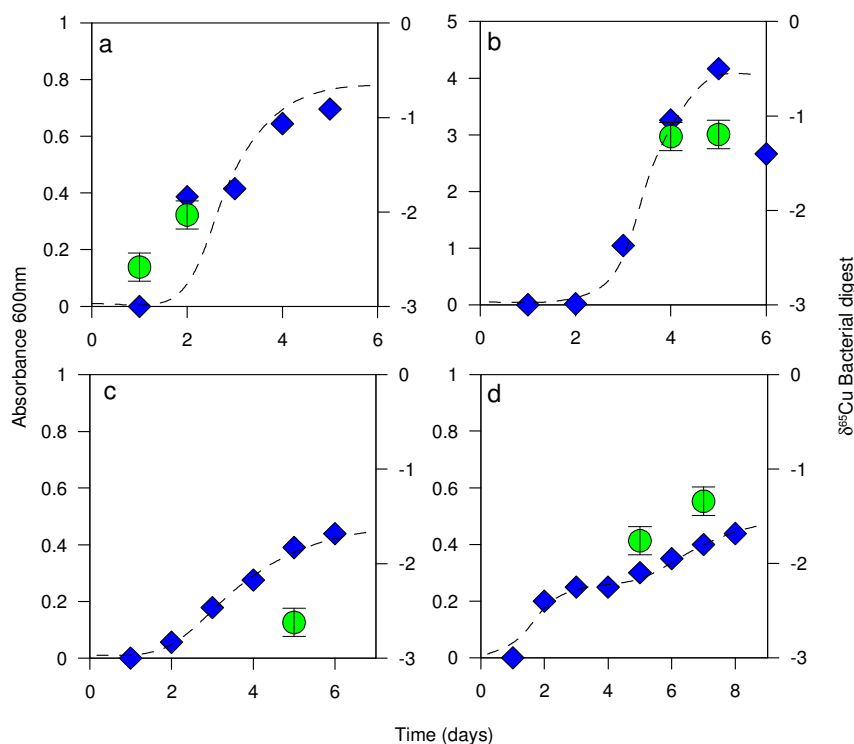


Figure 10. Absorbance at 600nm (blue diamonds) and $\delta^{65}\text{Cu}$ (green circles) data plotted as a function of time for intracellular incorporation experiments using (a) *E. coli*, (b) *B. subtilis*, (c) RGR consortium, and (d) CC consortium. Growth behavior is illustrated by a solid curve.

We calculated the $\Delta^{65}\text{Cu}_{\text{solution-solid}}$ for each of the metabolic experiments based on the fraction of Cu incorporated during growth and the $\delta^{65}\text{Cu}$ of the washed and digested bacterial pellets. *B. subtilis* and *E. coli* incorporated only a small fraction of the total Cu (<2%) and fractionated the Cu isotopes by an average of +1.2‰ and +2.3‰ ($\Delta^{65}\text{Cu}_{\text{solution-solid}}$, Eq.2), respectively. The RGR consortium incorporated almost 40% of the Cu in solution and fractionated the isotopes by +4.4‰ ($\Delta^{65}\text{Cu}_{\text{solution-solid}}$). The CC consortium incorporated 20% of the Cu in the solution and fractionated the isotopes by an average of +1.9‰ ($\Delta^{65}\text{Cu}_{\text{solution-solid}}$). The RGR and CC consortia contained several Gram-positive and Gram-negative bacterial species, but the RGR also contained large amounts of other microorganisms, including fungi and protozoa.

2.5 Sites of Cu Accumulation and Impact on Cell Morphology

We collected TEM images of *E.coli* cells used in the adsorption and intracellular uptake experiments to evaluate the impact of Cu on the cells and to help identify the sites of Cu-binding (Figures 11 a-b). Prior to Cu adsorption (Fig. 11a), *E. coli* cells looked “healthy” and had intact lipopolysaccharide (LPS) layers. After exposure to Cu, the LPS layer appears to be absent (Fig 11b). The polysaccharide chains of LPS extend outward for a distance of about 10 nm from the surface of the outer membrane, and the hydrophobic barrier made by the LPS is stabilized by structural cations such as Ca^{2+} and Mg^{2+} that link adjacent molecules via salt bridging (Beveridge and Koval 1981; Caroff and Karibian, 2003). The Cu in the experimental solution can displace the weakly bonded salt bridges, disrupting the LPS and outer membrane while leaving the integrity of the cell intact (e.g., Borrok et al., 2004). The location of adsorbed Cu is thought to be distinguished by the electron dense outer ring of the *E. coli* cells (Fig. 11b) which was not present in the control (Fig 11a). It appears that most Cu is associated with the *E.coli* surface and only small amounts of Cu likely penetrated inside the cell.

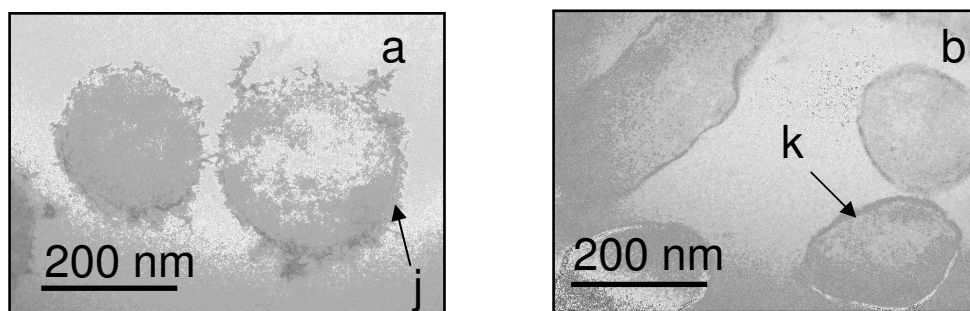


Figure 11. Transmission electron micrographs of (a) *E. coli* control with intact LPS (see arrow “j”) grown in TSB with 0.5% yeast extract and washed to remove residual media, and (b) *E. coli* after adsorption of Cu (II). The electron dense region (see arrow “k”) reflects Cu accumulation at the outer surfaces of cells.

Prior to Cu adsorption, *B. subtilis* cells had thick, intact cell walls coated with some EPS residue. Exposure to Cu apparently stressed the cells and in some cases of prolonged exposure induced sporulation. Figure 12 shows a TEM image of *B. subtilis* cells that were sporulating after exposure to Cu. Cu-induced sporulation of *Bacillus* cells has been documented previously by Kolodziej and Slepecky (1964). Copper (as indicated by the darker electron dense regions) appears to be sequestered between the outer coat of the spore and the inner membrane of the parent cell (Fig. 12). Ghosal et al. (2010) reported similar behavior for several monovalent metal cations which accumulated in the outer structures of *Bacillus* spores.

TEM images of *E. coli* cells before and after the intracellular uptake experiments (grown in basal media or basal media + Cu(II)-citrate), are presented in Figures 13a-b. Copper, represented by the electron dense material can be seen inside of all of the bacterial cells (Fig. 13b). This supports the observation that isotopic changes were related to intracellular uptake and not to surface reactions.

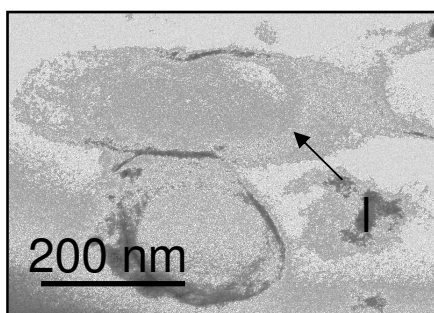


Figure 12. Transmission electron micrograph of *B. subtilis* cells in the process of sporulation. The electron dense region between the outer structure of the spores and the inner membrane of the parent cells reflects Cu accumulation (see arrow “I”).

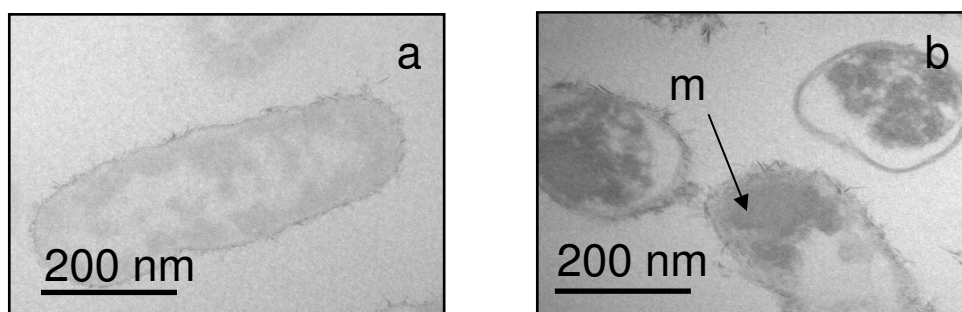


Figure 13. Transmission electron micrographs of (a) washed *E. coli* cells grown in basal media, and (b) *E. coli* grown in basal media amended with Cu-citrate. The image shows distinct electron-dense regions of Cu accumulation within the cells (see arrow “m”).

2.6 Mechanisms of Cu Isotope Fractionation

Although the distribution of Cu in the adsorption experiments is largely controlled by cell surface reactions, the fractionation of Cu isotopes appears to be controlled by active metabolic processes. The adsorption experiments with dead bacterial cells demonstrated that surface complexation with organic acid functional group sites alone did not substantially fractionate Cu isotopes. The latter result is similar to that reported by Pokrovsky et al. (2008) for Cu-bacteria adsorption experiments in

that no systematic isotopic variation was observed during surface adsorption experiments with most of the tested bacteria. Pokrovsky et al. (2008) suggested that the Cu bonding environment in aqueous solution was not substantially different (from a bond length/stiffness perspective) than the Cu bonds on the bacterial surface. They provide a review of available literature on Cu-organic acid bonding distances to support this position.

Cu adsorption experiments using live cells as well as active growth experiments with Cu(II)-citrate resulted in substantial isotopic fractionation of Cu, and the lighter Cu isotope was preferentially sequestered by the bacteria. This suggests that the mechanism of fractionation for both experimental types is generally similar. Isotopic fractionation of Cu is likely caused by the diffusion of Cu across the cell membrane and its subsequent binding to proteins inside the cell (some possibly involving the reduction of Cu(II) to Cu(I)). Because Cu is fundamental to cellular function in small concentrations but toxic at higher concentrations, the amount of Cu in cells is strictly regulated via dozens of proteins that can bind, chaperone, transport, reduce, and store Cu. Once Cu traverses the outer membrane of *E. coli* (possibly via porins), it is regulated by at least 5 homeostatic mechanisms involving specific Cu binding proteins housed in the periplasmic space and cytoplasm (Rensing and Grass, 2003). *B. subtilis* similarly regulates Cu through Cu chaperone proteins and efflux systems (e.g., Smaldone and Helmann, 2007). Our findings support the earlier work by Zhu et al. (2002) which demonstrated that specific Cu-binding proteins isolated from bacteria and yeast incorporated the lighter Cu isotope relative to the starting solution. Pokrovsky et al. (2008) described similar isotopic fractionation during Cu adsorption onto *P. aurofaciens* over the pH range 2 to 4; however, they attributed this to differences in bonding environment and not to metal diffusion or intracellular incorporation.

The apparent separation factors ($\Delta^{65}\text{Cu}_{\text{solid-solution}}$, Eq. 2) for all experimental data are presented in Figure 14. These data show a large degree of non-systematic variation in the magnitude of Cu isotope fractionation as they appear to be independent of pH and fraction adsorbed. This variability was also documented in the Pokrovsky et al. (2008) investigation and for different proteins in the Zhu et al.

(2002) investigation. Although the temptation with a highly-variable dataset is to dismiss its relevance, we believe that in this case the variability of the data is the relevance. Once we understand that the observed fractionations are not related to cell surface adsorption (this is why we refer to them as “apparent” separation factors), but are a reflection of active cellular function, variation in the magnitude of fractionation seems logical. The $\delta^{65}\text{Cu}$ is impacted not only by the types and abundances of bacterial Cu-binding proteins, which are be bacteria-specific, but also by the time of Cu exposure, the pH, and the degree of cell death, cell lysis, and in some cases sporulation (Fig. 12). Additional differences between the adsorption and intracellular incorporation experiments include the localities of Cu binding (Figures 11-13) and the availability of nutrients. Collectively, these observations suggest Cu isotopes are sensitive probes of complex intracellular Cu machinery and could be used as tools to understand and constrain these reactions.

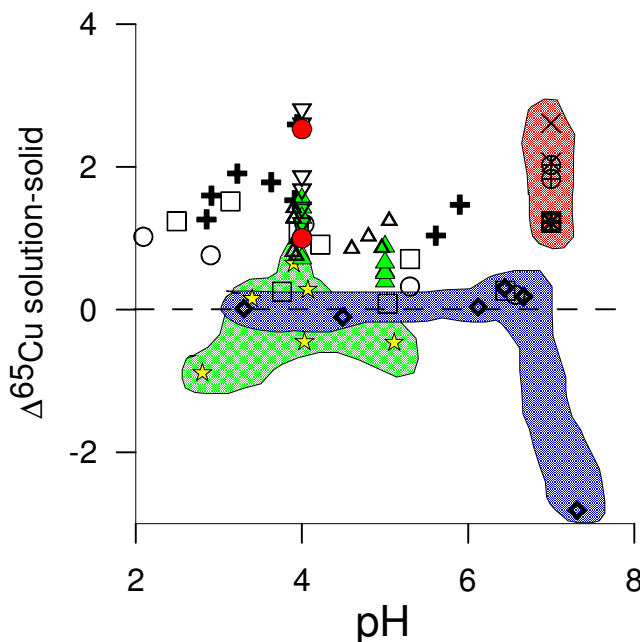


Figure 14. $\Delta^{65}\text{Cu}_{\text{solution-solid}}$ calculated via isotopic mass balance versus (a) the fraction of Cu adsorbed and (b) pH for all experiments.

Chapter 3: Conclusions

The fractionation of Cu isotopes by bacteria is a complex process that can be only partly constrained through bulk adsorption and intracellular uptake experiments. Additional experiments are needed that isolate Cu transport through the cell membrane into the periplasmic space and cytoplasm and that isolate Cu-binding by individual proteins. Future work should focus on linking Cu isotopic fractionation to these specific reactions and on spectroscopic work to constrain the bonding environments of internalized and surface-bound Cu. With this initial work, however, we can conclude the following:

1. Cu complexation with organic acid functional groups present on dead bacterial surfaces does not significantly fractionate the isotopes of Cu, but may exhibit a slight preference for the heavier Cu isotope. One key implication of this observation is that Cu complexation by the same organic-acid functional group sites associated with dissolved humic substances may not result in substantial fractionation either. Stronger Cu-organic ligand complexes may indeed fractionate Cu isotopes to a larger extent, but it seems likely that intracellular biological processes exert a primary control on the $\delta^{65}\text{Cu}$ of natural waters.
2. The behavior of Cu during bacterial surface interactions is more complex than previously thought based on Cu concentration data alone. Although the distribution of Cu in these experiments is controlled by surface adsorption, the isotopic changes suggest that some Cu enters the cells. At least in the case of *E. coli*, some of this Cu becomes irreversibly bound. Metal isotopic techniques can provide new insights into the mechanisms of binding environments associated with bacterial surface adsorption that were previously obscured in metal concentration data.
3. The magnitude and time-dependence of the Cu isotopic fractionation measured for the adsorption experiments with live cells is possibly a reflection of the metal diffusion rate across the intracellular membrane and/or a function of the available proteins within the internal Cu regulatory systems. If true, Cu isotopes might be used as a chemical tool to gather valuable toxicological information and

to learn about the mechanisms of Cu-bearing enzymes and proteins. Because there is structural and functional conservation between bacteria, yeast and humans (Peña et al., 1999), this tool could provide insights for several important biological systems.

4. Regardless of the experimental conditions (i.e., growth, media, species, form of Cu, etc.), live bacteria cells preferentially incorporated the lighter Cu isotope leaving the solution enriched in the heavy Cu isotope in all cases. Because abiotic reactions such as adsorption (e.g. Balistrieri et al., 2008; Pokrovsky et al., 2008) and precipitation (Fig. 1a) preferentially incorporate the heavier Cu isotope into the solid phase, we can identify a “biologic Cu isotope signature” in these simple systems. Although the additional complexities such as redox interactions in natural systems certainly play a complicating role, Cu isotopes appear to be well-suited tools for the discovery of biological markers on Earth or possibly other planets.

References

- Archer C., Vance D., Bermin J., Perkins J., Statham P. J., Lohan M. C., Ellwood M. J. and Mills R. A. (2008) The copper isotope geochemistry of rivers and the oceans. *Earth Plan. Sci. Lett.* **274**, 204-213.
- Asael D., Matthews A., Bar-Matthews M., Halicz L. (2007) Copper isotope fractionation in sedimentary copper mineralization (Timna Valley, Israel). *Chem. Geol.* **243**, 238-254.
- Ashworth D. J. and Alloway B. J. (2007) Complexation of copper by sewage sludge-derived dissolved organic matter: Effects on soil sorption behavior and plant uptake. *Water Air Soil Pollut.* **187**, 187-196.
- Balistrieri L. S., Borrok D. M., Wanty R. B., Ridley W. I. (2008) Fractionation of Cu and Zn isotopes during adsorption onto amorphous Fe(III) oxyhydroxide: Experimental mixing of acid rock drainage and ambient river water. *Geochim. Cosmochim. Acta* **72**, 311-328.
- Barling J. and Anbar A. D. (2004) Molybdenum isotope fractionation during adsorption by manganese oxides. *Earth. Planet. Sci. Lett.* **217**, 315–329.
- Beveridge T. J. (1989) Role of cellular design in bacterial metal accumulation and mineralization. *Rev. of Microbiol.* **43**, 147-171.
- Beveridge T. J. and Fyfe W. S. (1985) Metal fixation by bacterial cell walls. *Can. J. Earth Sci.* **22**, 1893-1898.
- Beveridge T. J. and Koval S. F. (1981) Binding of metals to cell envelopes of *Escherichia coli* K-12. *Appl. Env. Microbiol.* **42**, 325-335.
- Borrok D. and Fein J. B. (2004) Distribution of protons and Cd between bacterial surfaces and dissolved humic substances determined through chemical equilibrium modeling. *Geochim. Cosmochim. Acta* **68**, 3043-3052.

- Borrok D., Fein J.B., Tischler M., O'Loughlin E., Meyer H., Liss M., and Kemner K. (2004) The effect of acidic solutions and growth conditions on the adsorptive properties of bacterial surfaces. *Chem. Geol.* **207**, 107-119.
- Borrok D. M. and Fein J. B. (2005) The impact of ionic strength on the adsorption of protons, Pb, Cd, and Sr onto the surfaces of Gram negative bacteria: testing non-electrostatic, diffuse and triple-layer models. *J. Coll. Int. Sci.* **286**, 110-126.
- Borrok D. M., Wanty R. B., Ridley W. I., Wolf R., Lamothe P. J., Adams M. (2007) Separation of copper, iron, and zinc from complex aqueous solutions for isotopic measurement. *Chem. Geol.* **242**, 400-414.
- Brand L. E., Sunda W. G., Guillard R. L. (1983) Limitation of marine phytoplankton reproductive rates by zinc, manganese and iron. *Limnol. Oceanogr.* **28**, 1182-1198.
- Buchl A., Hawkesworth C. J., Ragnarsdottir K. V., Brown D. R. (2008) Re-partitioning of Cu and Zn isotopes by modified protein expression. *Geochem. Transact.* **9**:11 doi:10.1186/1467-4866-9-11.
- Caroff M. and Karibian D. (2003) Structure of bacterial lipopolysaccharides. *Carb. Res.* **338**, 2431-2447.
- Cheng K. J., Ingram J. M., Costerton J. W. (1970) Release of alkaline phosphatase from cells of *Pseudomonas aeruginosa* by manipulation of cation concentration and of pH. *J. Bact.* **104**, 748-753.
- Ehrlich S., Butler I., Halicz L., Richard D., Oldroyd A., Matthews A. (2004) Experimental study of the copper isotope fractionation between aqueous Cu(II) and covellite, CuS. *Chem. Geol.* **209**, 259-269.
- Fein J. B., Daughney C. J., Yee N., Davis T. A. (1997) A chemical equilibrium model for metal adsorption onto bacterial surfaces. *Geochim. Cosmochim. Acta* **61**, 3319-3328.
- Finney L. A. and O'Halloran T. V. (2003) Transition metal speciation in the cell: Insights from the chemistry of metal ion receptors. *Science* **300**, 931-936.
- Gauthier T. D., Seitz W. R., Grant C. L. (1987) Effects of structural and compositional variations of dissolved humic materials on pyrene Koc values. *Environ. Sci. Technol.* **21**, 243-248.

- Ghosal S., Leighton T. J., Wheeler K. E., Hutcheon I. D., Weber P. K. (2010) Spatially resolved characterization of water and ion incorporation in *Bacillus* spores. *Appl. Env. Microbiol.* **76**, 3275-3282.
- Green T. A., Russell A. E., Roy S. (1998) The development of a stable citrate electrolyte for the electrodeposition of copper-nickel alloys. *J. Electrochem. Soc.* **145**, 875-881.
- Gustafsson J. P. (2007) Visual MINTEQ, version 2.53. Web:
<http://www.lwr.kth.se/English/OurSoftware/vminteq/index.htm>
- Hersman L. E., Forsythe J. H., Ticknor L. O., Maurice P. A. (2001) Growth of *Pseudomonas mendocina* on Fe(III)(hydr)oxides. *Appl. Env Microbiol.* **67**, 4448-4453.
- Ivanov S. and Tsakova V. (2002) Influence of copper anion complexes on the incorporation of metal particles in polyaniline. Part I: Copper citrate complex. *J. Appl. Electrochem.* **32**, 701-707.
- Kimball B. E., Mathur R., Dohnalkova A. C., Wall A. J., Runkel R. L., Brantley S. L. (2009) Copper isotope fractionation in acid mine drainage. *Geochim. Cosmochim. Acta* **73**, 1247-1263.
- Koch K. A., Marjorette M., Peña M. M. O., Thiele D. J. (1997) Copper-binding motifs in catalysis, transport, detoxification and signaling. *Chem. Biol.* **4**, 549-560.
- Kolodziej B. and Slepecky R. A. (1964) Trace metal requirements for sporulation of *Bacillus Megaterium*. *J. Bacteriol.* **88**, 821-830.
- Larson P. B., Maher K., Ramos F. C., Chang Z., Gaspar M., Meinert L. D. (2003) Copper isotope ratios in magmatic and hydrothermal ore-forming environments. *Chem. Geol.* **201**, 337-350.
- Ma H., Kim S. D., Cha D. K., Allen H. E. (1999) Effect of kinetics of complexation by humic acid on toxicity of copper to *Ceriodaphnia dubia*. *Environ. Toxicol. Chem.* **18**, 28-837
- Markl G., Lahaye Y., Schwinn G. (2006) Copper isotopes as monitors of redox processes in hydrothermal mineralization. *Geochim. Cosmochim. Acta* **70**, 4215-4228.
- Mathur R., Ruiz J., Titley S., Liermann L., Buss H., Brantley S. (2005) Cu isotopic fractionation in the supergene environment with and without bacteria. *Geochim. Cosmochim. Acta* **69**, 5233-5246.

- Mathur R., Titley S., Barra F., Brantley S., Wilson M., Phillips A., Munizaga F., Maksaev V., Vervoort J., Hart G. (2009) Exploration potential of Cu isotope fractionation in porphyry copper deposits. *J. Geochem. Expl.* **102**, 1-6.
- Meador J. P. (1991) The interaction of pH, dissolved organic carbon, and total copper in the determination of ionic copper and toxicity. *Aquat. Toxicol.* **19**, 13.
- Pokrovsky O. S., Viers J., Enmova E. E., Kompantseva E. I., Freydier R. (2008) Copper isotope fractionation during its interaction with soil and aquatic microorganisms and metal oxy(hydr)oxides: Possible structural control. *Geochim. Cosmochim. Acta* **72**, 1742-1757.
- Peña M. M. O., Lee J., Thiele D. J. (1999) A delicate balance: Homeostatic control of copper uptake and distribution. *J. Nutr.* **129**, 1251-1260.
- Pribil M. J., Wanty, R. B., Ridley W. I., Borrok, D. M. (2010) Influence of sulfur-bearing polyatomic species on high precision measurements of Cu isotopic composition. *Chem. Geol.* **272**, 49-54.
- Rensing C. and Grass G. (2003) *Escherichia coli* mechanisms of copper homeostasis in a changing environment. *Microbiol. Rev.* **27**, 197-213.
- Smaldone G. T. and Helmann J. D. (2007) CsoR regulates the copper efflux operon *copZA* in *Bacillus subtilis*. *Microbiology* **153**, 4123-4128.
- Smith, R. M. and Martell, A. E. (1978) Critical stability constants. V. 1. Plenum Press, New York and London.
- Trevors J. T. and Cotter C. M. (1990) Copper toxicity and uptake in microorganisms. *J. Indust. Microbiol. Biotech.* **6**, 77-84.
- Wasylenki L. E., Anbar A. D., Liermann L. J., Mathur R., Gordon G. W., Brantley S. L. (2007) Isotope fractionation during microbial metal uptake measured by MC-ICP-MS. *J. Analyt. Atomic. Spectr.* **22**, 905-910.

Zhu X. K., Guo Y., Williams R. J. P., O’Nions R. K., Matthews A., Belshaw N. S., Canthers G. W., de Waal E. C., Weser U., Burgess B. K., Salvato B. (2002) Mass fractionation processes of transition metal isotopes. *Earth Planet. Sci. Lett.* **200**, 47-62.

Appendix

Copper isotope fractionation during adsorption and intracellular incorporation bacteria

Control experiment with Cu only, no bacteria

Sample ID	F precipitated	pH	d65Cu	n	d	2 sigma
21.2	0.40	6.44	1.077	2		0.105
21.3	0.01	3.30	0.722	1	1	0.193
21.5	0.05	6.12	0.748	1	1	
21.7	0.03	4.49	0.673	1	1	
21.9	0.58	6.67	1.130	2		0.112
21.10.	0.94	7.31	-1.308	2		0.049

E. coli adsorption vs. pH, 5g/L bacteria, 10 ppm Cu

Sample ID	F adsorbed	pH	d65Cu	n	d	2 sigma
Cu.8.1.U	0.21	2.79	0.719	1		
Cu.8.3.U	0.35	3.63	1.340	1		
Cu.8.5.U	0.39	3.91	1.307	1		
Cu.8.1.F	0.21	2.85	0.974	1		
Cu.8.3.F	0.24	2.91	1.097	2	2	0.152
Cu.8.6.F	0.84	5.61	1.580	1		
Cu.8.8.F	0.45	3.94	1.891	2		0.124
Cu.8.9.F	0.88	5.90	2.009	1		
Cu.8.10.F	0.43	3.22	1.524	1		

E. coli adsorption vs. pH, 15g/L bacteria, 2 ppm Cu

Sample ID	F adsorbed	pH	d65Cu	n	d	2 sigma
4B.1.Cu	0.95	6.45	0.943	1		
4B.2.Cu	0.64	4.22	1.276	1		
4B.3.Cu	0.90	5.30	1.333	1		
4B.4.Cu	0.93	5.03	0.770	1		
4B.5.Cu	0.45	2.49	1.253	1		
4B.6.Cu	0.72	3.76	0.873	1		
4B.7.Cu	0.80	3.96	1.565	1		
4B.8.Cu	0.67	3.14	1.703	1		

B. subtilis adsorption vs. pH, 5g/L bacteria, 10 ppm Cu

Sample ID	F adsorbed	pH	d65Cu	n	d	2 sigma
20.1	0.43	4.30	0.603	1		
20.2	0.27	2.09	0.629	1		
20.3	0.27	3.15	0.932	3	2	0.184
20.4	0.65	5.30	0.966	3	2	0.164
20.5	0.64	6.57	1.037	2	2	0.085
20.6	0.43	4.44	1.171	2		0.145
20.7	0.50	4.03	0.232	1		
20.8	0.17	2.90	0.704	1		

E. coli metal loading experiment

Sample ID	F adsorbed	pH	d65Cu	n	d	2 sigma
12.1.Cu.Load	0.43	4.00	1.046	2		0.070
12.2.Cu.Load	0.26	4.00	1.316	2		0.009
12.3.Cu.Load	0.13	4.00	1.281	2	2	0.289

B. subtilis metal loading experiment

Sample ID	F adsorbed	pH	d65Cu	n	d	2 sigma
31.1	0.19	4.00	1.254	1		

31.2	0.14	4.00	1.462	1		
31.3	0.07	4.00	1.387	1		
Heat-killed <i>E. coli</i> adsorption vs. pH, 5g/L bacteria, 10 ppm Cu						
Sample ID	F adsorbed	pH	d65Cu	n	d	2 sigma
40.2.Cu	0.27	2.80	0.417	2		0.108
40.3.Cu	0.38	3.40	0.750	1		
40.4.Cu	0.45	3.90	0.851	2		0.372
40.5.Cu	0.44	4.07	0.816	1		
40.6.Cu	0.45	4.03	0.399	2		0.260
40.8.Cu	0.75	5.11	0.341	2		0.014
48 hour kinetics experiment with <i>E. coli</i>						
Sample ID	F adsorbed	pH	d65Cu	n	d	2 sigma
39.1.Cu	0.22	4.30	1.265	1		
39.2.Cu	0.23	4.30	1.361	1		
39.3.Cu	0.28	4.30	1.811	1		
39.4.Cu	0.32	4.30	1.019	1		
39.5.Cu	0.36	4.30	1.370	1		
39.6.Cu	0.37	4.30	1.229	1		
39.7.Cu	0.52	4.30	1.325	1		
39.8.Cu	0.55	4.30	1.618	2		0.131
<i>E. coli</i> kinetics and reversibility experiment						
Sample ID	F adsorbed	pH	d65Cu	n	d	2 sigma
11.1.Cu.Kin	0.17	4.00	0.669	2		0.098
11.2.Cu.Kin	0.18	4.00	0.981	2		0.150
11.3.Cu.Kin	0.20	4.00	0.860	2		0.486
11.4.Cu.Kin	0.19	4.00	0.762	1		
11.6.Cu.Kin	0.18	4.00	0.511	2		0.072
11.7.Cu.Kin	0.21	4.00	1.478	3	2	0.063
11.8.Cu.Kin	0.22	4.00	0.525	2		0.088
11.9.Cu.Kin	0.20	4.00	0.948	1		
11.10.Cu.Kin	0.44	5.00	0.903	2		0.170
11.11.Cu.Kin	0.41	5.00	0.947	1		
11.12.Cu.Kin	0.44	5.00	0.955	1		
11.14.Cu.Kin	0.45	5.00	1.028	1		
11.15.Cu.Kin	0.45	5.00	1.130	1		
11.16.Cu.Kin	0.35	4.00	0.894	2		0.032
11.17.Cu.Kin	0.31	4.00	0.672	1		
11.18.Cu.Kin	0.31	4.00	1.203	1		
11.19.Cu.Kin	0.29	4.00	1.373	1		
11.20.Cu.Kin	0.28	4.00	0.862	1		
11.21.Cu.Kin	0.29	4.00	0.988	1		
11.22.Cu.Kin	0.29	4.00	0.652	1		
11.23.Cu.Kin	0.35	4.00	1.179	1		
<i>B. subtilis</i> kinetics and reversibility experiment						
Sample ID	F adsorbed	pH	d65Cu	n	d	2 sigma
30.1	0.42	3.93	1.034	1		
30.2	0.43	3.93	1.140	1		
30.3	0.43	3.90	1.263	2		0.047
30.4	0.43	3.89	1.065	1		
30.5	0.72	4.96	1.332	1		
30.6	0.72	4.80	1.452	1		
30.7	0.73	5.05	1.622	2		0.190

30.8	0.65	4.60	1.267	1	
30.9	0.41	3.90	1.236	1	
30.10.	0.45	3.90	1.351	2	0.127
<i>E. coli</i> intracellular Cu					
	F Cu SOLID	pH	d65 SOLID		
EC 1	0.01	7.00	-3.045	1	
EC 2	0.02	7.00	-2.493	1	
<i>B. subtilis</i> intracellular Cu					
	F Cu SOLID	pH	d65 SOLID		
BS 1	0.01	7.00	-1.680	1	
BS 2	0.02	7.00	-1.658	1	
Rio Grande Reservoir consortia intracellular Cu					
	F Cu SOLID	pH	d65 SOLID		
RGB 1	0.40	7.00	-3.085	1	
Cement Creek consortia intracellular Cu					
	F Cu SOLID	pH	d65 SOLID		
NB 9/24 2	0.13	7.00	-2.222	2	0.027
NB 9/26 1	0.27	7.00	-1.804	1	
Atomic adsorption standard					
AA std				15	0.712 0.140
Copper rod standard					
Cu ROD				12	0.716 0.166

Curriculum Vita

Jesica Urbina Navarrete was born in Chicago, Illinois on March 25, 1978 to Maria C. Urbina. She graduated from Bel-Air High School in El Paso, TX in May 1996. Jesica attended the University of Texas at El Paso from 2004-2010 where she obtained a Bachelor of Science degree in Microbiology with a minor concentration in Chemistry and a Master of Science in Environmental Science. During her undergraduate studies she worked as a research assistant with Dr. Emily Haltiwanger on type II diabetes research and during her graduate career she has expanded her work to include environmental research. Her thesis, *Copper isotope fractionation during surface adsorption and intracellular incorporation by bacteria*, has been submitted for publication in the scientific journal, *Geochimica et Cosmochimica Acta*. Jesica has earned academic recognition as the recipient of multiple academic scholarships to include: the NSF Graduate Research Fellowship Award 2010-2013, MS PHD's in Earth System Science Professional Development Program, Cohort VII, 2010-2011, LSAMP Recipient – Louis Stokes Alliance for Minority Participation Fellow Jan 2009-Jan 2011, Southwest Association of Hispanic American Physicians Academic Excellence scholarship recipient, Spring 2008, UTEP College of Science Dean's List, Fall 2007, University Honors Program, Fall 2004-Spring 2006, and the Wolslager Foundation Scholarship recipient, Spring 2004. Jesica has also worked as a research assistant for various NSF, NIH and internationally funded research projects and has been a participant in national and international scientific meetings. Jesica has been accepted into the doctoral program in Geological Sciences at the University of Texas at El Paso where she will continue her research in near-surface biogeochemistry.

Permanent address: 5733 Hasan Ave
El Paso, TX 79924

This thesis/dissertation was typed by Jesica Urbina Navarrete.